3D laser imaging by backprojection

Jean-Baptiste Bellet, Gérard Berginc

3D LASER IMAGING BY BACKPROJECTION

JEAN-BAPTISTE BELLET AND GÉRARD BERGINC

Abstract. In this paper, we are interested in imaging a 3D scene from a collection of 2D laser images, using advanced tomographic methods. We first recall classical results about transmission tomography, including the famous FDK algorithm for cone-beam scanning. Then we use a pinhole camera model to describe the laser experiment of interest. Since this model is geometrically speaking similar with the cone-beam scanning, we use the FDK algorithm as a heuristic to reconstruct the scene. We show numerically, on real data, that this heuristic reconstructs the skeleton of an object to be imaged, even if the object is occulted.

1. Introduction

A new imaging technic of three-dimensional laser imaging has emerged from the industrial community [3–5]. The aim is to reconstruct a three-dimensional scene from a collection of two-dimensional laser images. These laser images are obtained by a laser emitter, which illuminates the observed scene in the visible or near-infrared band. The laser radiation reflected by the different objects is collected by a high-pixel density detector to give a two-dimensional image. One sub-question is identifying an object from the scene, which may contain occultations. This laser system can provide high resolution images, which can enhance three-dimensional object recognition. New scientific and industrial challenges have arised from this imaging method. These challenges include the need of an efficient mathematical algorithm, specially dedicated for such industrial laser data.

This subject belongs to imaging by wave propagation: receivers measure the effect of a medium on waves emitted by sources, and the goal is to produce an image of the medium from recorded data. Here we furthermore assume that the source is a laser emitting in the visible or near-infrared band (from 500 nm to 2200 nm). We also assume that the collected data contain the backscattered intensity of the incident laser pulse. This essential characteristic annihilates hopes of using standard imaging methods such as seismic or radar methods, since they are based on the travel times. Also surfaces of the scene are supposed to be rough, *i.e.* they are not locally plane surfaces comparing with the wavelength. Then physical phenomena involve diffusion and methods of [2] cannot be applied. The 2D recorded images are supposed to be monostatic: they are measured by a 2D array of receivers which is close to the source. Repeating the experiment for different source positions yields a collection of 2D images, which needs to be treated to get a 3D reconstruction of the original scene. This formulation recalls the two following problems. The first one is the stereographic problem: reconstructing a 3D scene from several photographies. But stereoscopy assumes a model of lambertian diffusion and weak occultations. These assumptions may be violated in our case, which concerns a technique of laser imagery with the ability to identify targets at very long ranges; so we will not use stereographic methods.

The second one is the Computed Tomography (CT) coming from X-ray scanners in medical imaging: reconstructing a 3D object from 2D slices measured by scanning the object with X-rays. Let us mention that the relevant methods were also recently used in the visible spectrum, under the name of Optical Projection Tomography (OPT) [8]. Then the idea of using these transmission tomographic methods in the infrared spectrum has been introduced in [3–5]. In this paper we propose to recall classical results about transmission tomography, to explain how using CT for the laser configuration of interest, and then to test this method on real data.

Let us first recall transmission tomography, using the excellent mathematical references [1, 7]. The cone-beam scanning experiment is the following: a source turns on a circle around a scene.

Date: November 13, 2013; v2.1bis.

2010 *Mathematics Subject Classification.* 94A08; 65R10; 78A97.

Key words and phrases. Laser imaging; transmission tomography; filtered backprojection; FDK algorithm.

Acknowledgement. This work was partially supported by the Agence pour les Mathématiques en Interaction avec l'Entreprise et la Société, under Grant ANR-10-LABX-0002-01.

It scans the scene by emitting non-diffracting radiation in the medium such as X-rays for the human body. A 2D receptor array is tangent to the circle on the antipodal point of the source. Each receptor measures the attenuated intensity through the medium. It gives the integral of an attenuation coefficient, over the line through the source and the considered receptor. If we restrict this experiment to the plane which contains the circle we get a 2D configuration called linear fan-beam scanning. For that 2D case, measurements yield directly some discretization of the Radon transform of the attenuation. So they can be inverted using a filtered backprojection algorithm. Basically, for each pixel, we compute a contribution from all lines through this pixel and a source, and we then sum all these contributions. This gives the unknown attenuation coefficient, pixel by pixel. The ingenious FDK algorithm [6] uses this 2D fan-beam formula to approach the 3D cone-beam inversion. Indeed, for each voxel, a line through a source and the voxel is included in a plane which intersects the receptor array on a line which is parallel to the circle plane. We can compute the contribution of this line as if the problem were restricted to this 2D plane, using of course the 2D fan-beam formula. Then, even if these planes are different when the source moves, we sum all the contributions from all such lines, as if they were in embedded in the same 2D plane. The result is a volume, computed voxel by voxel, which is the so-called FDK reconstruction.

Let us come back to the laser problem. A laser source turns around a 3D scene. At each position, it illuminates the scene, and a receptor array measures the backscattered light in a focal plane in the monostatic configuration. Recorded data form a set of 2D images related to backscattered intensity, resulting from an interaction of the laser beam with surfaces of the scene. We need a model. In our paper, we propose the following one: we use a pinhole camera model to describe geometrically the acquisition. We interpret a laser image as a projection of the scene, along rays converging to a same point: the optical center of the optical recording instrument. This acquisition model is geometrically speaking very similar with the cone-beam scanning. This is an empirical reason to use the FDK algorithm to backproject laser data in order to get a reconstruction of the scene. There is a slight difference to be precised: laser data are not transmission tomography data. As a result it is not completely obvious that the FDK algorithm works, and it is used as an extension, or a heuristic, rather than an exact inversion method. We then show numerically the relevance of this approach. We display slices of the reconstructed volumes; we also show that extracting a sub-volume whose FDK reconstruction is between two levels yields a skeleton of the object to be identified.

This paper is organized as follows. We first recall some results about the transmission tomography: from the Radon transform and its inversion by a filtered backprojection to the FDK algorithm for cone-beam scanning; this first part finishes with numerical illustrations. Then we present the use of CT for laser data, from the pinhole camera model to the extraction of a skeleton of the object, with the FDK algorithm as an intermediate step. This method is tested using real data, including a case of an object with occultations. We conclude this paper by some open questions.

2. Transmission tomography

2.1. **Radon inversion by filtered backprojection.**

2.1.1. *Radon transform.* The mathematical basis of the transmission tomography is the Radon transform $\mathcal{R}$, which basically consists in integrating over hyperplanes. In a 2D set-up, a hyperplane is a line $L(\theta, s) = \{x \in \mathbb{R}^2 : x \cdot \theta = s\}$, where $\theta \in S^1$ is a unitary vector which is orthogonal to the line and $s \in \mathbb{R}$ is the signed distance from the origin to the line. Thus the Radon transform of a function f is defined by

$$\mathcal{R}[f](\theta, s) := \int_{L(\theta,s)} f \mathrm{d}\ell \text{ (where } \ell \text{ denotes the length measure).}$$

The most natural way to measure such a transform is to realize the transmission tomography experiment in the standard parallel scanning geometry: for each angular position θ, a source moves along a line directed by θ and illuminates the scene along a line orthogonal to θ, of the form $L(\theta, s)$. A receptor which moves at the same time behind the object measures $\mathcal{R}[f](\theta, s)$. Thus such an experiment collect projections along sets of parallel lines of the form $L(\theta, s), s$.

2.1.2. *Main results about the Radon transform.* The Radon transform satisfies several properties following its behavior under the Fourier transform and convolution. Let $\mathcal{F}_x$ be the 2D-Fourier transform on the x-variable and let $\mathcal{F}_s$ be the 1D-Fourier transform on the s-variable:

$$\mathcal{F}_x[f(x)](\xi) = (2\pi)^{-1}\int_{\mathbb{R}^2} f(x)\mathrm{e}^{-\mathrm{i}x\cdot\xi}\mathrm{d}x, \quad \mathcal{F}_s[g(\theta,s)](\theta,\sigma) = (2\pi)^{-1/2}\int_{\mathbb{R}} g(\theta,s)\mathrm{e}^{-\mathrm{i}s\sigma}\mathrm{d}s.$$

We can also define two convolution products (on x or s, depending on context):

$$(f_1 * f_2)(x) = \int_{\mathbb{R}^2} f_1(x-y)f_2(y)\mathrm{d}y, \quad (v*g)(\theta,s) = \int_{\mathbb{R}} v(\theta,s-t)g(\theta,t)\mathrm{d}t.$$

Then the central slice theorem links the Radon transform with the Fourier transform:

$$\mathcal{F}_s[\mathcal{R}[f](\theta,s)](\theta,\sigma) = (2\pi)^{1/2}\mathcal{F}_x[f](\sigma\theta);$$

this implies :

$$\mathcal{R}[f_1 * f_2] = \mathcal{R}[f_1] * \mathcal{R}[f_2].$$

The adjoint operator $\mathcal{R}^*$ of the Radon transform is called the backprojection operator. It acts on functions $g(\theta,t)$ in this way:

$$\mathcal{R}^*[g](x) = \int_{S^1} g(\theta, x\cdot\theta)\mathrm{d}\theta.$$

This operation consists in integrating over lines through x. This backprojection operator can be written in the Fourier domain: for g satisfying the symmetry property $g(\theta,s) = g(-\theta,-s)$,

$$\mathcal{F}_x\left[\mathcal{R}^*g\right](\xi) = 2(2\pi)^{1/2}\left|\xi\right|^{-1}\mathcal{F}_s[g]\left(\frac{\xi}{|\xi|},|\xi|\right). \tag{2.1}$$

The backprojection operator gives the inversion formula of the Radon transform:

$$\mathcal{R}^*\left[\mathcal{H}\frac{\partial}{\partial s}\mathcal{R}f(\theta,s)\right] = 4\pi f, \tag{2.2}$$

where the operator $\mathcal{H}$ is the Hilbert transform, *i.e.* the convolution by $\mathrm{p.v.}\frac{1}{\pi s}$. More generally, a filtered backprojection of $g(\theta,s)$ is of the form $\mathcal{R}^*[v*g]$, where v is a filter. A filtered backprojection operator acts on the Radon transform in this way:

$$\mathcal{R}^*[v*\mathcal{R}f] = \mathcal{R}^*[v]*f. \tag{2.3}$$

This formula is the basis of the filtered backprojection algorithm.

2.1.3. *Filtered backprojection.* To reconstruct f from the knowledge of its Radon transform $\mathcal{R}f$, the idea of this algorithm is indeed to compute the filtered backprojection $\mathcal{R}^*[v*\mathcal{R}f]$ of the data, where $v(s)$ is a symmetric filter such that its backprojection $\mathcal{R}^*[v]$ is close to a Dirac distribution, and thus (2.5) is close to f. To design an algorithm which reconstructs faithfully functions f of bandwidth 2Ω, we choose a filter v_Ω such that $\mathcal{R}^*[v_\Omega]*f = f$ for f such that $\mathcal{F}_x[f](\xi) = 0, |\xi| \geqslant \Omega$; with the help of (2.1), we see in Fourier domain that this is the case for v_Ω satisfying:

$$\mathcal{F}_x\left[\mathcal{R}^*v_\Omega\right](\xi) = 2(2\pi)^{1/2}\left|\xi\right|^{-1}\mathcal{F}_s[v_\Omega](|\xi|) = (2\pi)^{-1}\mathbb{1}_{|\xi|\leqslant\Omega},$$

More generally, we allow $v_\Omega(s)$ such that:

$$\mathcal{F}_s[v_\Omega](\sigma) = 2^{-1}(2\pi)^{-3/2}\left|\sigma\right|\hat{\varphi}(\sigma/\Omega), \tag{2.4}$$

where $\hat{\varphi}(\nu)$ is a cutoff function close to $\mathbb{1}_{|\nu|\leqslant 1}$. This expression for v_Ω has to be compared with the inversion formula (2.2): up to a constant factor, $|\sigma|$ is the Fourier expression of the operator $\mathcal{H}\frac{\partial}{\partial s}$; so the filter (2.4) is just the filter of the inversion formula combined with a low-pass filter. Different choices of the cutoff $\hat{\varphi}$ yield different possible filters. For example, $\hat{\varphi}(\nu) = \mathbb{1}_{|\nu|\leqslant 1}$ yields the Ram-Lak filter; another example is the Shepp-Logan filter, with $\hat{\varphi}(\nu) = \mathbb{1}_{|\nu|\leqslant 1}\operatorname{sinc}\frac{\nu\pi}{2}$ (where $\operatorname{sinc}\nu := \frac{\sin\nu}{\nu}$).

The next step to design the algorithm is to discretize the filtered backprojection $\mathcal{R}^*[v*\mathcal{R}f]$ to compute it from a discrete set of data. This is precisely the aim of the next subsection for linear fan-beam data.

2.2. **Imaging from linear fan-beam data.** As a preliminary step to 3D-imaging from cone-beam scanning data, we consider linear fan-beam data; such data are cone-beam scanning data restricted to the plane containing the trajectory of the source.

We assume that a 2D-scene to be imaged is in the disk $|x| < \rho$: the unknown is an attenuation coefficient f supported in this disk. A source runs on the circle $|x| = r$ with $\rho \ll r$. When the source is on $r(\cos\beta, \sin\beta) = r\theta(\beta)$, it scans the object by emitting rays; a receptor array records the attenuated intensity on the antipodal point of the source position. The measurement from the ray through $r\theta$ and $y\theta_\perp(\beta) = y(\sin\beta, -\cos\beta)$ yields the integral of f over this line; it is denoted by $g(\beta, y)$. See Figure 1. Of course, g is the Radon transform of f with other coordinates:

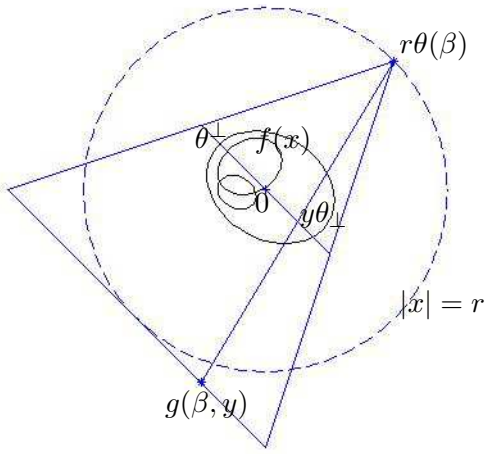

FIGURE 1. Tomography by fan-beam scanning: the measurement $g(\beta, y)$ is the line integral of the attenuation $f(x)$, over the ray through the source $r\theta(\beta)$ and the (virtual) point $y\theta_\perp(\beta) \in \theta^\perp$.

$$g(\beta, y) = \mathcal{R}f(\Theta(\beta, y), s(y)), \qquad \text{with } \Theta(\beta, y) = \begin{pmatrix} \cos(\beta + \arctan\frac{y}{r} - \frac{\pi}{2}) \\ \sin(\beta + \arctan\frac{y}{r} - \frac{\pi}{2}) \end{pmatrix}, s(y) = \frac{ry}{(r^2 + y^2)^{1/2}}.$$

We assume g to be sampled on a regular grid:

$$\beta_j = j\Delta\beta, \Delta\beta = \frac{2\pi}{p}, j = 0, \dots, p-1,$$
$$y_l = (l + \delta)\Delta y, l = -q, \dots, q,$$

where δ is the detector set-off and is either 0 or $\pm 1/4$. We choose q such that the whole reconstruction region $|x| < \rho$ is covered by the rays. Assuming that f is (essentially) Ω-band-limited, we assume the following sampling conditions:

$$\Delta y \leqslant \frac{\pi}{\Omega}, \quad \Delta\beta \leqslant \frac{r + \rho}{r}\frac{\pi}{\Omega\rho}.$$

To apply the filtered backprojection algorithm to these data $g(\beta_j, y_l)$, the idea is to write the filtered backprojection $\mathcal{R}^*[v_\Omega * \mathcal{R}f] = \mathcal{R}^*[v_\Omega] * f$ of f with the new (β, y)-coordinates in the integrals. After some simplifications, and some approximation based on the assumption $\rho \ll r$, we get:

$$\mathcal{R}^*[v_\Omega] * f(x) = \int_{S^1} \frac{r^2}{(r - x\cdot\theta)^2} h\left(\beta, \frac{rx\cdot\theta_\perp}{r - x\cdot\theta}\right) \mathrm{d}\theta, h(\beta, z) = \int_{-\rho}^{\rho} v_\Omega(z - y)\, g(\beta, y) \frac{r\mathrm{d}y}{(r^2 + y^2)^{1/2}}. \tag{2.5}$$

The first step is to compute the $h(\beta_j, y_k)$ using a trapezoidal rule: for $j = 0, \dots, p-1$, for $k = -q, \dots, q$, we compute the discrete convolution

$$h_{j,k} := h(\beta_j, y_k) = \Delta y \sum_{l=-q}^{q} v_\Omega(y_k - y_l) g(\beta_j, y_l) \frac{r}{(r^2 + y_l^2)^{1/2}}.$$

The second step is to compute the weighted backprojection, using a linear interpolation to estimate $h(\beta_j, z)$ from the $h_{j,k}$, and using a trapezoidal to compute the integral: for each reconstruction

point x (on a regular grid of pixels), we estimate $f(x)$ by computing

$$f_{\mathrm{FB}}(x) = r^2 \Delta\beta \sum_{j=0}^{p-1} \frac{1}{(r - x\cdot\theta_j)^2} \left[(1-\omega)h_{j,k} + \omega h_{j,k+1}\right];$$

here, with $\theta_j = \theta(\beta_j)$ and $\theta_{j,\perp} = \theta_\perp(\beta_j)$, we have chosen $\frac{rx\cdot\theta_{j,\perp}}{r-x\cdot\theta_j} = (1-\omega)y_k + \omega y_{k+1}$, with $t = \frac{rx\cdot\theta_{j,\perp}}{r-x\cdot\theta_j}\frac{1}{\Delta_y} - \delta$, $k = \lfloor t \rfloor$, $\omega = t - k$.

The sampling conditions justify that integrals are precisely evaluated with the use of the trapezoidal rules; so the method has resolution Ω.

2.3. **Imaging from cone-beam scanning.** We consider the 3D imaging problem from cone-beam scanning data; it is a 3D-extension of the 2D linear fan-beam. We present the FDK algorithm which is a very famous heuristic to solve this 3D imaging problem. The approximation is based on using ingeniously the 2D linear fan-beam inversion.

We assume that a 3D-scene to be imaged is determined by an unknown attenuation coefficient f supported in the ball $|x| < \rho$. A source runs on a circle $|x| = r$ in the horizontal plane $x_3 = 0$, with $\rho \ll r$. When the source is on $r(\cos\beta, \sin\beta, 0) = r\theta(\beta)$, it scans the object by emitting rays. A receptor array is on the antipodal point, in the plane $-r\theta + 2\theta^\perp$; it records the attenuated intensity. To simplify the parametrization, we interpret the plane $\theta^\perp$ as a screen on which we see this recorded image. The measurement from the ray through $r\theta$ and $y = y_2\theta_\perp + y_3 e_3 \in \theta^\perp$, with $\theta_\perp(\beta) = (\sin\beta, -\cos\beta, 0)$ and $e_3 = (0,0,1)$, yields the integral of f over the ray; it is denoted by $g(\beta, y)$. Then g is the ray transform of f; it is also seen that the 2D linear fan-beam is here exactly the cone-beam restricted to the horizontal plane. See Figure 2.

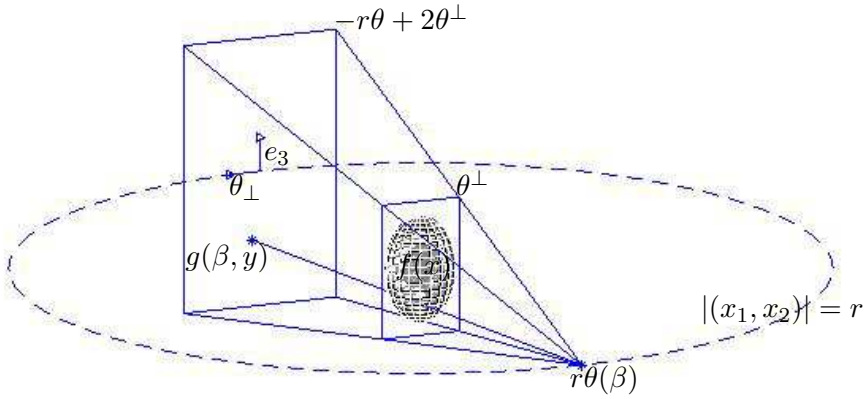

FIGURE 2. Tomography by cone-beam scanning: the measurement $g(\beta, y)$ is the line integral of the attenuation $f(x)$, over the ray through the source $r\theta(\beta)$ and the point $y = y_2\theta_\perp + y_3 e_3$ in the (virtual) screen $\theta^\perp$.

The line through the source position $r\theta(\beta)$ and a point x hits the screen $\theta^\perp$ at $y_2\theta_\perp + y_3 e_3$, where:

$$y_2 = \frac{r}{r - x\cdot\theta} x\cdot\theta_\perp, \quad y_3 = \frac{r}{r - x\cdot\theta} x_3. \tag{2.6}$$

Let $\pi(x,\theta)$ be the plane through $r\theta$ and x that intersects the screen $\theta^\perp$ on the horizontal line $\mathbb{R}\theta_\perp + y_3 e_3$. If the experiment were a 2D-linear fan-beam scanning in the plane $\pi(x,\theta)$, we would have to consider the contribution of the fan-beam inversion formula which belongs to θ, and then to integrate over θ to get the final estimation of $f(x)$. The idea of the FDK algorithm is to extend this by computing the integral of contributions from the 2D-inversion formula, disregarding the fact that contributions from different θ come from different planes.

We consider the point $y_3 e_3$ as origin in $\pi(x,\theta)$. We denote x' the coordinates of x in $\pi(x,\theta)$: $x' = x - y_3 e_3$; the angle θ' to be considered in $\pi(x,\theta)$ is $\theta' = (r\theta - y_3 e_3)/r'$, where $r' = (r^2 + y_3^2)^{1/2}$ is the distance from $r\theta$ to the origin in $\pi(x,\theta)$. Then, we read from the inversion formula (2.5) that the contribution which belongs to θ' is:

$$I(x,\theta) = \frac{r'^2}{(r' - x'\cdot\theta)^2} \int_{-\rho}^{\rho} v_\Omega\left(\frac{r'x'\cdot\theta_\perp}{r' - x'\cdot\theta'} - y_2'\right) g(\beta, y_2'\theta_\perp + y_3 e_3) \frac{r'\mathrm{d}y_2'}{(r'^2 + {y_2'}^2)^{1/2}}.$$

This is the contribution from the direction θ' in $\pi(x,\theta)$ to the filtered backprojection. To estimate $f(x)$ by the 2D backprojection algorithm in $\pi(x,\theta)$, we need to integrate all contributions from all directions in $\pi(x,\theta)$. But this is impossible since the source moves in the horizontal plan instead of $\pi(x,\theta)$. The idea of the FDK algorithm is to integrate over the contributions from the sources that we have:

$$f(x) \sim f_{\mathrm{FDK}}(x) = \int I(x,\theta)\mathrm{d}\theta'.$$

After some computations, we get the FDK formula:

$$f_{\mathrm{FDK}}(x) = \int_{S^1} \frac{r^2}{(r - x\cdot\theta)^2} h(\beta, y)\mathrm{d}\theta, h(\beta,y) = \int_{-\rho}^{\rho} v_\Omega\left(y_2 - y_2'\right) g(\beta, y_2'\theta_\perp + y_3 e_3) \frac{r\mathrm{d}y_2'}{(r^2 + y_2'^2 + y_3^2)^{1/2}}. \tag{2.7}$$

Here, we recall that $y = y_2\theta_\perp + y_3 e_3$ is the projection on the screen $\theta^\perp$ of the point x, along the line through the source $r\theta(\beta)$ (y_2 and y_3 are given by (2.6)). The FDK formula (2.7) is similar with the fan-beam formula (2.5); we discretize it in a similar way. We assume that we know $g(\beta, y)$ on a regular grid: data are a 3D matrix under the form $[g(\beta_j, y_{2,l}, y_{3,k})]_{j,l,k}$; here, the pixels of the 2D-screen are the $(y_{2,l}, y_{3,k})$. First, we compute h on the grid: $[h(\beta_j, y_{2,l}, y_{3,k})]_{j,l,k}$; we weight the data by $\frac{r}{(r^2+y_2'^2+y_3^2)^{1/2}}$, and then we compute a discrete convolution. Then we compute the discrete weighted backprojection $f_{\mathrm{FDK}}(x)$ for each reconstruction point x on a 3D-grid (set of voxels). Let us notice that this procedure needs interpolation on the 2D-screen; we use linear interpolation for each coordinate y_2 and y_3. To speed up the computations it is useful to notice that voxels on a vertical line share the same horizontal interpolation coefficients.

2.4. **Numerical results.** To illustrate the above approaches, we have simulated data for both 2D and 3D cases. The classical class of objects being used for such simulations are Shepp-Logan phantoms: linear combinations of charasteristic functions of ellipsoids. Integrating over lines such attenuation functions reduces to a geometrical problem whose solution is a closed formula: compute the length of intersection of a line and ellipsoids. Thus the involved ray transforms can be computed exactly.

We have represented on the Figure 3 two sinograms: the left one represents fan-beam data $g(\beta_j, y_l)$, where β_j moves horizontally and y_l moves vertically, the right one is the filtering of weighted data: $h(\beta_j, y_l)$. Then we have represented on the Figure 4 two attenuation coefficients:

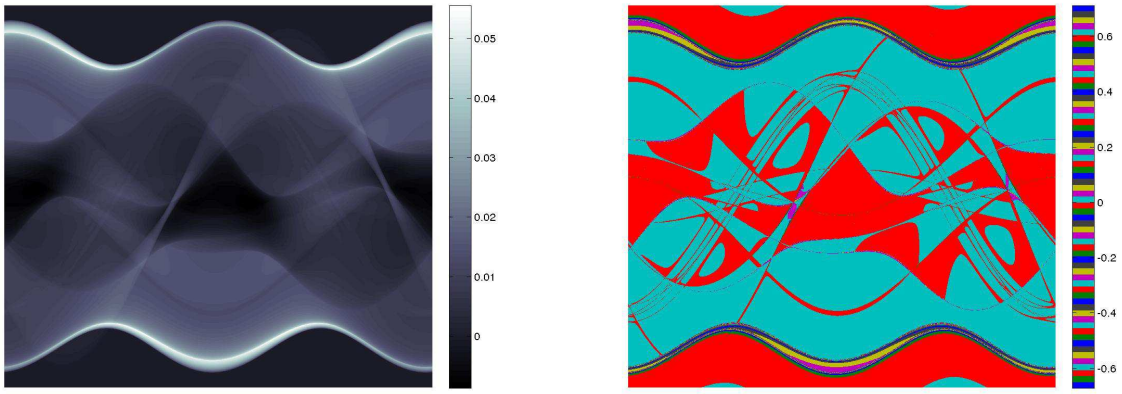

FIGURE 3. fan-beam sinogram g (left) and its weighted filtering h (right).

the left one is the Shepp-Logan phantom f that has been used to generate the fan-beam data, the right one is the reconstruction image f_{FB} that we get after backprojecting h. Similarly, we have represented on the Figure 5 slices of a 3D sinogram $g(\beta_j, y_{2,l}, y_{3,k})$ associated with a cone-beam scanning simulation. Here, one projection image (associated with one source position β) is a slice in a plane of constant β. Then we have represented on the Figure 6 two volumic attenuation coefficients: the top one is the Shepp-Logan phantom f that has been used to generate the cone-beam data, the bottom one is the reconstruction volume f_{FDK} that we get using the FDK algorithm.

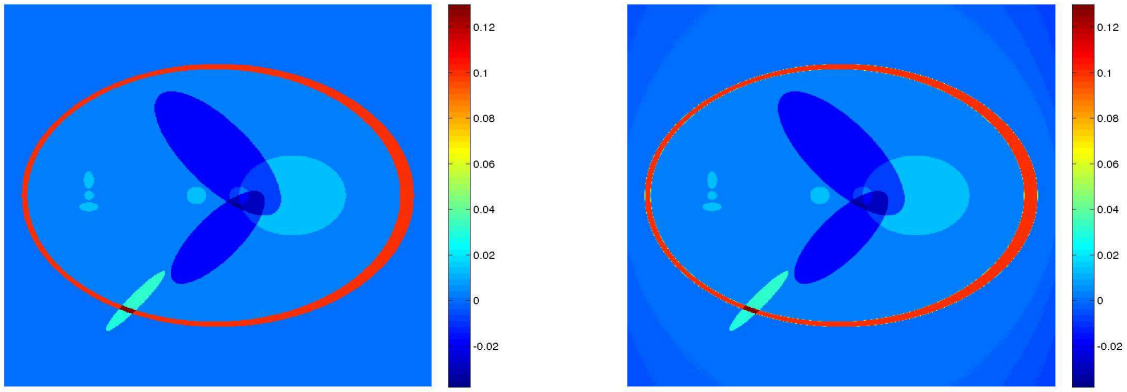

FIGURE 4. A 2D Shepp-Logan phantom f (left) and its reconstruction f_{FB} by filtered backprojection (right).

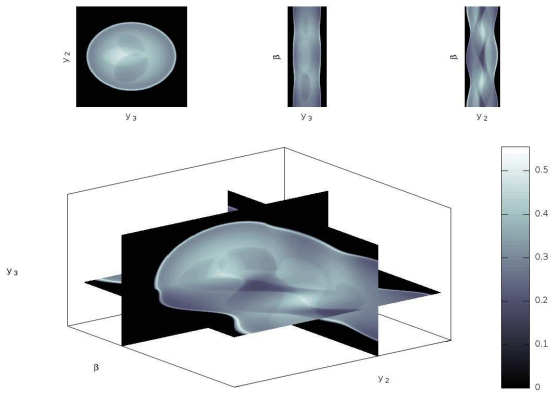

FIGURE 5. Slices of cone-beam data $g(\beta, y_2, y_3)$.

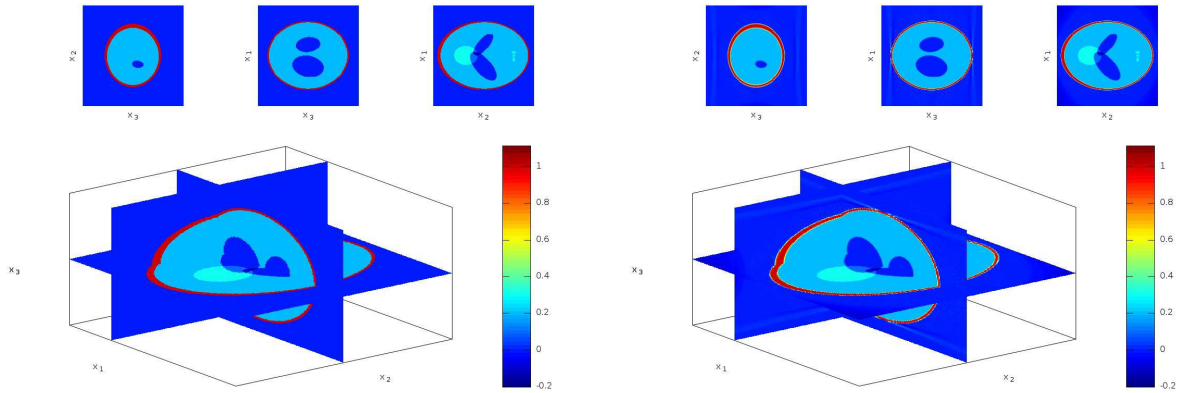

FIGURE 6. Slices of a 3D Shepp-Logan phantom f (left) and its reconstruction f_{FDK} by the FDK algorithm (right).

3. Heuristic for 3D laser imaging

3.1. **Laser images.** We now assume that a laser source turns around a 3D scene, running on a circle whose center is the origin. The scene may contain an object with or without occultations. At

each position, the laser illuminates the scene, and a receptor array measures the backscattered light in a focal plane, in the monostatic configuration. We get in this way a set of 2D intensity images consisting of reflection data, resulting from an interaction of the laser beam with surfaces of the scene. The aim is to reconstruct the 3D scene from these 2D images.

In the sequel we consider that a laser image is designed according to an optical model: the pinhole camera model; see Figure 7. After a laser illumination each object point of the scene reemits in many directions. An optical instrument is used to record the data. It contains a receptor plane which is (parallel to) the tangent plane of the circle, and it is assumed to refocused rays coming from a same object point to a same image point in the receptor plane; this image point is aligned with some optical center of the recording instrument and the object point. As a result a laser image is a projection of the scene along rays through the optical center. So the acquisition geometry is exactly a cone-beam scanning geometry as the transmission tomography one!

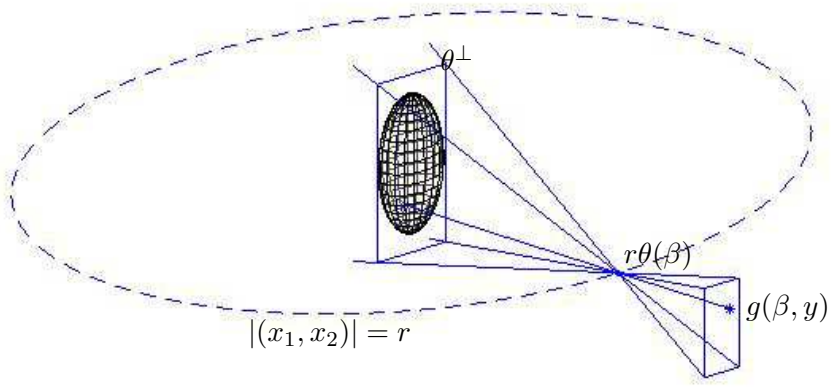

FIGURE 7. Pinhole camera model: a visible point from the scene is projected on the receptor array along the line through the optical center $r\theta(\beta)$ of the device. The measurement is $g(\beta, y)$, where the line intersects the virtual screen $\theta^\perp$ on $y = y_2\theta_\perp + y_3 e_3$.

Let us now specify the analogous notations. The optical center of the recording instrument runs on a circle of radius r in the horizontal plane $x_3 = 0$. Its current position is $r(\cos\beta, \sin\beta, 0) = r\theta(\beta)$. The receptor array is included in a plane which is parallel to $\theta^\perp$ and which is close to $r\theta(\beta)$. Here again we can imagine that the projections are observed in a virtual screen located in the plane $\theta^\perp$. The measurement $g(\beta, y)$ from the ray through $r\theta$ and $y = y_2\theta_\perp + y_3 e_3 \in \theta^\perp$, with $\theta_\perp(\beta) = (\sin\beta, -\cos\beta, 0)$ and $e_3 = (0, 0, 1)$, concerns the closest point of the scene (from $r\theta$) which belongs to the ray. The main difference with the usual tomography is: for the transmission tomography the measurement $g(\beta, y)$ was an integral over the ray; here this property has been lost.

To finish the description of the acquisition geometry, we need to write the discrete version that we get in practical situations. Data are given under the form of a 3D-matrix: $[g(\beta_j, y_{2,l}, y_{3,k})]_{j,l,k}$. First, we assume that images are uniformly distributed on half-a-circle, *i.e.* the angles are $\beta_j = j\Delta\beta, \Delta\beta = \frac{\pi}{p}, j = 0, \ldots, p$. Then we assume that the discretization of the virtual screen is the regular 2D-grid $(y_{2,l}, y_{3,k})_{l,k}$ which is supposed to be centered on the origin. Then we see that up to rescalings, we can assume that the horizontal step $y_{2,l+1} - y_{2,l}$ is $\delta_y = 1$ and that the vertical step $y_{3,k+1} - y_{3,k}$ is $\delta_z = 1$. To completely determine the rays we have now to explicit the radius r of the circle after these rescalings. The apparent size S of the observed scene is the ratio of the horizontal size of the array over the distance from the array to the optical center. The apparent size S depends only on the recording optical instrument and is supposed to be known. By the way the Thales theorem claims that the apparent size S is also equal to the ratio of the horizontal size L of the virtual screen over the distance r from the screen to the optical center. After the above rescalings, S does not change and L becomes the number of horizontal pixels (of a recorded image) minus one. Then the radius of the circle becomes $r = SL$. If it is needed to work with real scales, then the steps δ_y and δ_z (before rescalings) must also be known.

Using the analogy with tomographic data, laser data can be represented within a sinogram. Two examples of such real sinograms have been represented on the Figures 8 and 9. The first one concerns an object without occultations whereas the second one is an object with occultations.

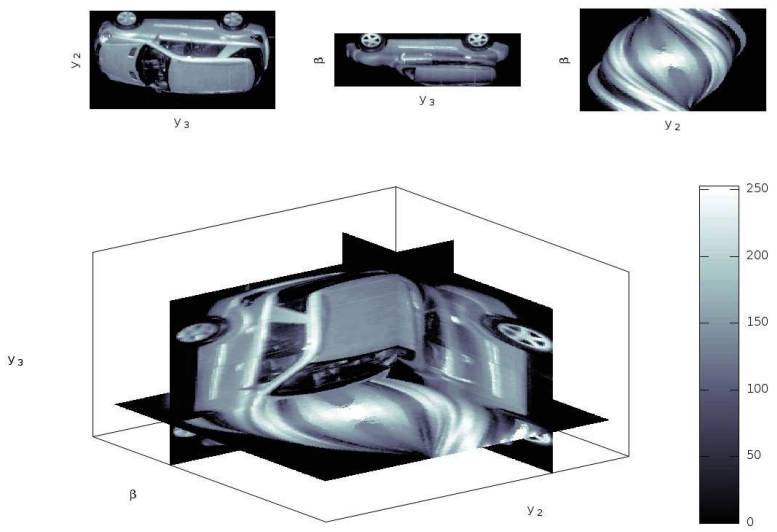

FIGURE 8. Slices of a laser sinogram; example 1: object without occultations.

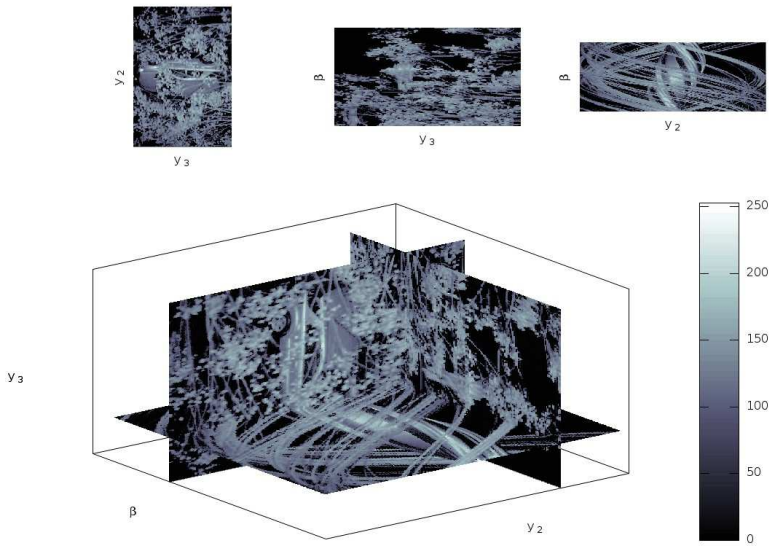

FIGURE 9. Slices of a laser sinogram; example 2: object with occultations.

3.2. **Backprojection of laser images.** We have modelled the acquisition geometry of laser images as the cone-beam scanning geometry. Thus some idea to recover the scene is applying a filtered backprojection algorithm from transmission tomography. Thus we apply the FDK algorithm with a laser sinogram as input. Since no mathematical proof has so far related laser images with the ray transform, it cannot be rigorously stated that this method determines a function representing completely the scene. So the sequel must be considered as numerical tests of the FDK algorithm, used as a heuristic for laser images inversion.

The FDK reconstructions have been computed for the above examples. They have been represented under a slices view form on Figures 10 and 11 (on left). In both cases we get some representation of the scene as a 3D volume. Some levels of this FDK volume are located near the reflecting surfaces of the scene, including the object itself and the occultations.

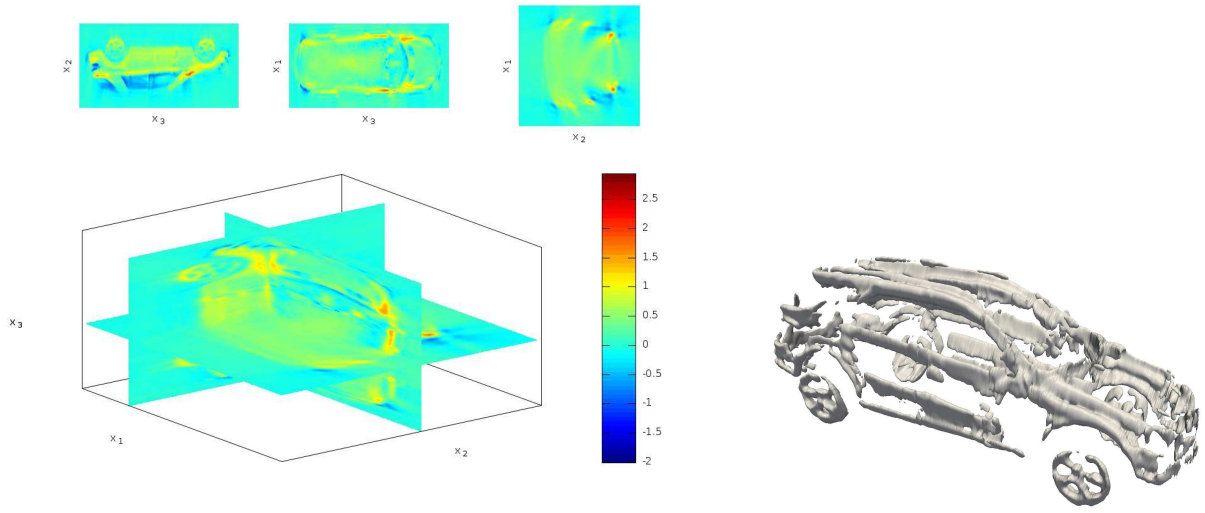

FIGURE 10. FDK reconstruction for the laser sinogram 1 (object without occultations): slices (left) and isovolume (right).

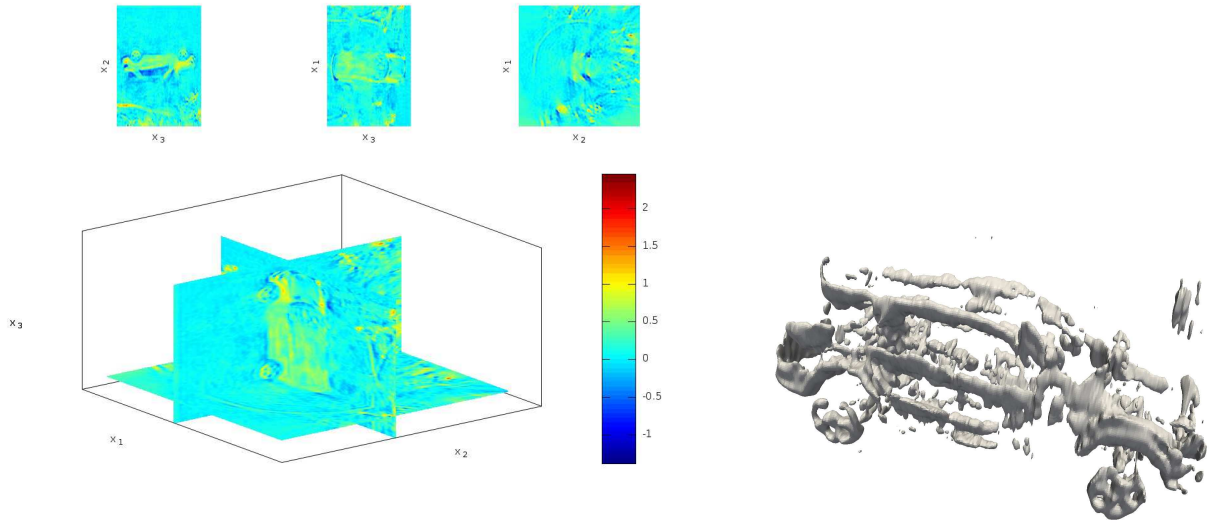

FIGURE 11. FDK reconstruction for the laser sinogram 2 (object with occultations): slices (left) and isovolume (right).

Another important point is being able to extract the object from this volume. A simple idea is to manually identify a small box which contains the object and then to extract points from this box whose FDK value is between two chosen levels. We can get (with the isovolume function of the Paraview software) in this way the representations (on right) of Figures 10 and 11. We empirically observe that such a representation contains some skeleton of the original object, containing what we could call *singularities*: edges or interfaces between different pieces. This is true for the object without occultations; this is also true for the object with occultations, even if of course the result is better without occultations.

4. Conclusion and open questions

Filtered backprojection algorithms were designed to invert Radon kind transforms, which correspond traditionally to data from the transmission tomography. In this paper we have modelled the formation of laser images using the pinhole camera model; then we have applied a filtered backprojection method (FDK algorithm) to real laser images, as a heuristic. We have observed that it yields interesting 3D reconstructions, even for objects with occultations.

A mathematical gap must be filled, because we have used data resulting from laser interactions with surfaces. The data collected by the focal plane detector correspond to laser intensity scattered by the randomly rough surfaces of the illuminated objects. An open question is then finding a proof which justifies why a filtered backprojection algorithm works well with such reflection data. Such a proof might relate laser data with the Radon transform. Filling this mathematical gap may also identify the limits of the method, and may help to design filters more efficient than the tomographic ones.

References

[1] H. Ammari. *An Introduction to Mathematics of Emerging Biomedical Imaging*. Springer, 2008.
[2] J.-B. Bellet and G. Berginc. Imaging from monostatic scattered intensities. *M2AS*, 2013.
[3] G. Berginc and M. Jouffroy. Simulation of 3D laser systems. In *Geoscience and Remote Sensing Symposium, 2009 IEEE International, IGARSS 2009*, volume 2, pages 440–444. IEEE, 2009.
[4] G. Berginc and M. Jouffroy. Simulation of 3D laser imaging. *PIERS Online*, 6(5):415–419, 2010.
[5] G. Berginc and M. Jouffroy. 3D laser imaging. *PIERS Online*, 7(5):411–415, 2011.
[6] L. Feldkamp, L. Davis, and J. Kress. Practical cone-beam algorithm. *JOSA A*, 1(6):612–619, 1984.
[7] F. Natterer and F. Wübbeling. *Mathematical methods in image reconstruction*. SIAM, 2007.
[8] J. Sharpe. Optical projection tomography as a new tool for studying embryo anatomy. *Journal of anatomy*, 202(2):175–181, 2003.

Universite de Lorraine, Institut Elie Cartan de Lorraine, UMR 7502, Metz, F-57045, France, CNRS, Institut Elie Cartan de Lorraine, UMR 7502, Metz, F-57045, France.
E-mail address: jean-baptiste.bellet@univ-lorraine.fr

Thales Optronique, 2, Avenue Gay Lussac CS 90502, 78995 Élancourt Cedex, France.
E-mail address: gerard.berginc@fr.thalesgroup.com